




Maternal nutrient restriction during pregnancy and lactation leads to impaired right ventricular function in young adult baboons

Anderson H. Kuo¹ , Cun Li^{2,3}, Hillary F. Huber² , Matthias Schwab⁴, Peter W. Nathanielsz^{2,3} and Geoffrey D. Clarke^{1,3} 

¹Department of Radiology and Research Imaging Institute, University of Texas Health Science Center at San Antonio, San Antonio, TX, USA

²Department of Animal Science, University of Wyoming, Laramie, WY, USA

³Southwest National Primate Research Center, San Antonio, TX, USA

⁴Hans Berger Department for Neurology, University Hospital, Jena, Germany

Key points

- Maternal nutrient restriction induces intrauterine growth restriction (IUGR) and leads to heightened cardiovascular risks later in life.
- We report right ventricular (RV) filling and ejection abnormalities in IUGR young adult baboons using cardiac magnetic resonance imaging.
- Both functional and morphological indicators of poor RV function were seen, many of which were similar to effects of ageing, but also with a few key differences.
- We observed more pronounced RV changes compared to our previous report of the left ventricle, suggesting there is likely to be a component of isolated RV abnormality in addition to expected haemodynamic sequelae from left ventricular dysfunction. In particular, our findings raise the suspicion of pulmonary hypertension after IUGR.
- This study establishes that IUGR also leads to impairment of the right ventricle in addition to the left ventricle classically studied.

Abstract Maternal nutrient restriction induces intrauterine growth restriction (IUGR), increasing later life chronic disease including cardiovascular dysfunction. Our left ventricular (LV) CMRI studies in IUGR baboons (8 M, 8 F, 5.7 years – human equivalent approximately 25 years), control offspring (8 M, 8 F, 5.6 years), and normal elderly (OLD) baboons (6 M, 6 F, mean 15.9 years) revealed long-term LV abnormalities in IUGR offspring. Although it is known that right ventricular (RV) function is dependent on LV health, the IUGR right ventricle remains poorly studied. We examined the right ventricle with cardiac magnetic resonance imaging in the same cohorts. We observed decreased ejection fraction (49 ± 2 vs. $33 \pm 3\%$, $P < 0.001$), cardiac index (2.73 ± 0.27 vs. 1.89 ± 0.20 l min⁻¹ m⁻², $P < 0.05$), early filling rate/body surface area (BSA) (109.2 ± 7.8 vs. 44.6 ± 7.3 ml s⁻¹ m⁻², $P < 0.001$), wall thickening (61 ± 3 vs. $44 \pm 5\%$, $P < 0.05$), and longitudinal shortening (26 ± 3 vs. $15 \pm 2\%$, $P < 0.01$) in IUGR animals with increased chamber volumes. Many, but not all, of these changes share similarities to normal older animals. Our findings suggest IUGR-induced pulmonary hypertension should be further investigated and that atrial volume, pulmonic outflow and interventricular septal motion may provide valuable insights into IUGR cardiovascular physiology. Overall, our findings reaffirm that gestational and neonatal challenges can result in long-term programming of poor offspring cardiovascular health. To our knowledge, this is the first study reporting IUGR-induced programmed adult RV dysfunction in an experimental primate model.

(Received 15 December 2016; accepted after revision 3 April 2017; first published online 25 April 2017)

Corresponding author A. H. Kuo: Department of Radiology, University of Texas Health Science Center at San Antonio, 7703 Floyd Curl Drive, MC 7800, San Antonio, TX 78229-3900, USA. Email: kuoa@uthscsa.edu

Abbreviations BSA, body surface area; CMRI, cardiac magnetic resonance imaging; CO, cardiac output; CVD, cardiovascular disease; ED, end diastolic; EDV, end diastolic volume; ESV, end systolic volume; EF, overall ejection fraction; eFR, early filling rate; ER, ejection rate; ES, end systolic; FR, overall filling rate; IUGR, intrauterine growth restriction; LSF, longitudinal shortening fraction; LV, left ventricular; MNR, maternal nutrient restriction; pWT, peak wall thickness; RV, right ventricular; SI, sphericity index; SV, stroke volume; WTF, wall thickening fraction.

Introduction

The intrauterine environment is a major determinant of fetal health. Associations between many teratogens and fetal abnormalities, such as those seen in fetal alcohol syndrome, which occurs following excessive maternal alcohol consumption during pregnancy, have long been known (Clarren & Smith, 1978). It is now clear from extensive human epidemiological and experimental animal studies that physiological challenges to the pregnant mother, such as decreased nutrition or over-nutrition, are also associated with predisposition of offspring to a wide variety of long-term health complications. These changes produced by gene–environment interactions are known as developmental programming and have led to the concept of the ‘developmental origins of health and disease’ (Godfrey *et al.* 2007). Most remarkably, offspring of mothers undernourished in early pregnancy during periods of famine exhibited increased incidence of dyslipidaemia and cardiovascular disease (CVD), whereas offspring of mothers in later stages of pregnancy during the period of limited nutrient availability exhibited higher incidence of glucose intolerance (Roseboom *et al.* 2001). Low birth weight (a hallmark of intrauterine growth restriction; IUGR) has been linked to increased incidence of CVD, stroke, hypertension, diabetes, osteoporosis, and an assortment of multi-systemic dysfunctions in humans (Fowden *et al.* 2006). Various components of those changes have been replicated in animal models, suggestive of a causal relationship (Armitage *et al.* 2004). Yet, the mechanisms underlying these predispositions remain poorly understood.

Using cardiac magnetic resonance imaging (CMRI), we have reported left ventricular (LV) functional decrease in IUGR offspring born to baboons that ate 70% of the global diet of mothers eating *ad libitum* during pregnancy and lactation (Kuo *et al.* 2016). In that study, decreased LV ejection fraction (EF), filling rate, cardiac index and wall thickening were present in IUGR offspring with increased spherical morphology and chamber volume, similar to alterations seen in older animals and closely resembling characteristics of early, subclinical heart failure. These worrying cardiac changes are thought to contribute to the elevated CVD risk seen later in life as a result of decreasing cardiac reserve. Yet, the cardiac left ventricle is hardly an isolated organ. Given the interdependence of the cardiac chambers, we sought to determine whether

right ventricular (RV) function was also impaired in the IUGR offspring.

Animal studies show that approximately 20–40% RV pressure and outflow result from LV contraction (Yamaguchi *et al.* 1991) via interventricular modulation of overall ventricular deformation and wall stress (Santamore & Dell’Italia, 1998). Clinically, patients with left sided heart failure often show concomitant right-sided cardiac dysfunction (Drazner *et al.* 1998; Voelkel *et al.* 2006). Significant failure of the systemic cardiac chambers also inevitably propagates upstream, increasing the work required for pulmonary perfusion, leading to pulmonary hypertension (Oudiz, 2007; Lam *et al.* 2009b). RV contractile impairment and elevated afterload from pulmonary hypertension are frequently observed in heart failure patients, especially in severe cases (Kalogeropoulos *et al.* 2011; Segers *et al.* 2012). Importantly, RV dysfunction has been proposed as a strong predictor of mortality in patients with heart failure (Polak *et al.* 1983; de Groote *et al.* 1998; Melenovsky *et al.* 2014). Based on our previous LV findings paralleling mild degree of heart failure, we hypothesized that RV dysfunction also occurs in IUGR baboon offspring and may be detected by CMRI.

Methods

Ethical approval

All procedures were approved by the Texas Biomedical Research Institute Institutional Animal Care and Use Committees (IACUC) and conducted in facilities approved by the Association for Assessment and Accreditation of Laboratory Animal Care. The IACUC is accredited by the Association for Assessment and Accreditation of Laboratory Animal Care International. This work complies with the animal ethical principles under which *The Journal of Physiology* operates and with the checklist outlined by Grundy (2015).

Animal model

Baboons (*Papio* species) were group housed and maintained in a social environment and fed using an individual feeding system (Schlabritz-Loutsevitch *et al.* 2004). Healthy gravid female baboons of similar age and weight were randomly assigned to an *ad libitum* diet or a globally reduced diet regimen consisting of 70% of feed eaten by control *ad lib* fed mothers on a

Table 1. Baseline characteristics of subjects studied (mean \pm SD)

Characteristic	CTL		OLD		IUGR	
	M	F	M	F	M	F
<i>n</i>	8	8	6	6	8	8
Age (years)	5.3 \pm 1.4	5.7 \pm 1.3	18.5 \pm 2.2	13.4 \pm 1.5	5.9 \pm 1.2	5.5 \pm 1.4
Weight (kg)	19.5 \pm 6.8	13.9 \pm 2.1	31.4 \pm 7.5	17.2 \pm 2.2	21.6 \pm 4.3	13.4 \pm 1.2
Calculated body surface area (m ²)	0.55 \pm 0.13	0.44 \pm 0.04	0.77 \pm 0.12	0.51 \pm 0.04	0.60 \pm 0.08	0.44 \pm 0.03
Heart rate (bpm)	95 \pm 7	108 \pm 17	89 \pm 8	97 \pm 13	91 \pm 16	94 \pm 15
Birth weight (kg)	0.93 \pm 0.14	0.89 \pm 0.10	NA	NA	0.82 \pm 0.08	0.74 \pm 0.14

NA, not available.

weight-adjusted basis from 0.16 gestation (G) to end of lactation (Li *et al.* 2013). The offspring baboons were fully weaned at 9 months of age and moved to juvenile group housing, where *ad lib* diet was given. They were fed Monkey Diet 5038 (Purina LabDiets, St Louis, MO, USA) containing 13% calories from fat, 18% calories from protein, 69% calories from carbohydrates, mineral and vitamin additives, and a metabolizable energy content of 3.22 kcal g⁻¹.

Cardiac magnetic resonance imaging

CMRI was performed on three groups of baboons: young adult IUGR baboons (IUGR, *n* = 16, 8 male, age = 5.7 \pm 1.3 years; mean \pm SD), age-matched control baboons (CTL, *n* = 16, 8 male, age = 5.6 \pm 1.3 years), and elderly adult baboons (OLD, *n* = 12, 6 male, age = 15.9 \pm 3.1 years). We previously studied and reported decrease of LV function in these same animals (Kuo *et al.* 2016). To account for potential diurnal and prandial effects on cardiovascular function, the studies were always conducted the same time of the day, in the morning (09.00–12.00 h) after overnight fast. Subject baseline data are shown in Table 1.

Cardiac MRI was accomplished under general anaesthesia. Anaesthesia was induced with ketamine hydrochloride (12 mg kg⁻¹, i.m.) and maintained with isoflurane (0.8–1.0%, inh). Oral intubation was performed following anaesthesia induction for mechanical ventilation. Subsequently, cannulation of the right saphenous vein for i.v. access was performed. Body temperature was maintained with a custom built feedback-regulated circulating water blanket. Continuous physiological parameter monitoring was performed as well as visual assessment for respiration, movement and mucosal coloration. Mechanical ventilation was performed at approximately 10 strokes min⁻¹ and 120–180 ml stroke⁻¹. In sequence acquisitions where breath hold was required, a brief interval of hyper-ventilation was performed followed by a brief period of ventilation suspension, not exceeding 30 s in duration,

followed by prompt resumption of ventilation support. Mechanical ventilation and physiological monitoring were performed using MRI-compatible equipment.

All studies were performed on a 3.0 Tesla MR scanner (TIM Trio, Siemens Healthcare, Malvern, PA, USA) with a six-channel anterior phased-array torso coil and corresponding posterior coil elements, resulting in an aggregate of up to 12 channels of data. Before each imaging session, a standard quality control phantom was scanned to ensure geometric accuracy, spatial resolution and contrast were within acceptable limits. CMRI was performed using steady-state free precession sequences. A 3D breath-held localizer was first obtained to allow for imaging-plane planning. High temporal resolution cine images with retrospective gating (TR/TE 3.0/1.5 ms, 25 cardiac phases, matrix 144 \times 192, FOV 188 \times 250 mm²) were then obtained. A stack of 20–24 contiguous short-axis slices (2.5 mm thickness, no gap) was acquired serially during repetitive breath-holds at end expiration. A stack of gated, breath-held four-chamber long-axis slices (5–10 slices centred around the ventricular apex) was also obtained.

On conclusion of the CMRI study, inhalational isoflurane was discontinued, and the subject slowly weaned to room air and transported to the recovery area. Measurements of heart rate, EKG, temperature, blood pressure, *P*_{O₂}, and end-tidal CO₂ were continued. Upon extubation, visual assessment of the animal for respiration, mucosal coloration and movement was performed at regular intervals not exceeding 15 min in duration until the animal was alert, in a sternal position and demonstrated control of movement. After full recovery, baboons were returned to their home cage.

Image processing and analysis

The CMR⁴² image analysis package (Circle Cardiovascular, Calgary, AB, Canada) was used for CMR data analysis. Endocardial contour of the right ventricle was traced using a semiautomatic algorithm in a time-resolved manner, yielding a working RV model (Fig. 1). RV end

diastolic (ED) and RV end systolic (ES) phases were determined by maximal and minimal cavum volumes with visual confirmation, which matched LV-ES and ED phases. RV-EF was computed using RV-EDV and RV-ESV. Average RV ejection and filling rates (ER, FR) were calculated by standard formulas. RV early filling rate (eFR) was determined by rate of RV volume change in the pre-diastasis period, visually considered based on the ventricular filling curve, which averaged to approximately the first 150 ms of diastole (6/25 cardiac phases). Longitudinal length of the right ventricle was manually measured from the tricuspid plane to the chamber apex using long-axis images. RV longitudinal shortening fraction (LSF) was defined as change in long axis length between systole and diastole divided by the diastolic length. The RV sphericity indices (SI) at end-systole and end-diastole (RV-ESSI, RV-EDSI) were calculated as chamber volume at end-systole and end-diastole divided by a theoretical sphere formed by the long axis length at the respective cardiac phase (Kim *et al.* 2006). Wall thickness was measured at the level of the mid-ventricular cavity in the lateral free wall at end-systole and end-diastole. To account for regional variability in wall thickness, measurements were taken from visually selected representative positions of the free wall within the slices, obtained from three consecutive slices, and averaged. RV wall thickening fraction (RV-WTF) was calculated as the difference between the systolic and diastolic wall thickness divided by the systolic wall thickness.

Normalization

Parameters based on dimensional measurements were evaluated with reference to the body surface area (BSA), estimated using weight-based models as previously

described for baboons (Glassman *et al.* 1984; VandeBerg *et al.* 2009). For females:

$$\text{BSA}[\text{m}^2] = 0.078 (\text{weight}[\text{kg}])^{0.664}$$

and in males,

$$\text{BSA}[\text{m}^2] = 0.083 (\text{weight}[\text{kg}])^{0.639}.$$

Thus, for instance, RV cardiac index (RV-CI) was defined as the amount of blood pumped by the heart per minute per square metre of body surface area.

Statistical analysis

Data were analysed using R 3.2.1 statistical software (R Foundation for Statistical Computing, Vienna, Austria) and Prism 6 (GraphPad Software, La Jolla, CA, USA). Grubbs's test (extreme Studentized deviate) was used to evaluate for statistical outliers. Outliers were excluded from analysis. Normality of distribution was assessed by the d'Agostino–Pearson test. Two-way ANOVA was used to evaluate the null hypotheses that there were no differences between the factors group and sex and no significant interactions. *Post hoc* multiple comparison correction was performed using Tukey's honest significance test, giving adjusted (*post hoc*) *P* values.

To examine whether RV functional status can be linked to the extent of intrauterine growth, correlation analysis was performed between RV-EF and birth weight as well as RV early filling rate (eFR) and birth weight. To determine if the filling function and ejection function change in concert, correlation analysis between those two parameters was performed. Similarly, correlation analysis was performed between the previously reported LV-EF and RV-EF from the current study to determine whether these values change in parallel. Additionally,

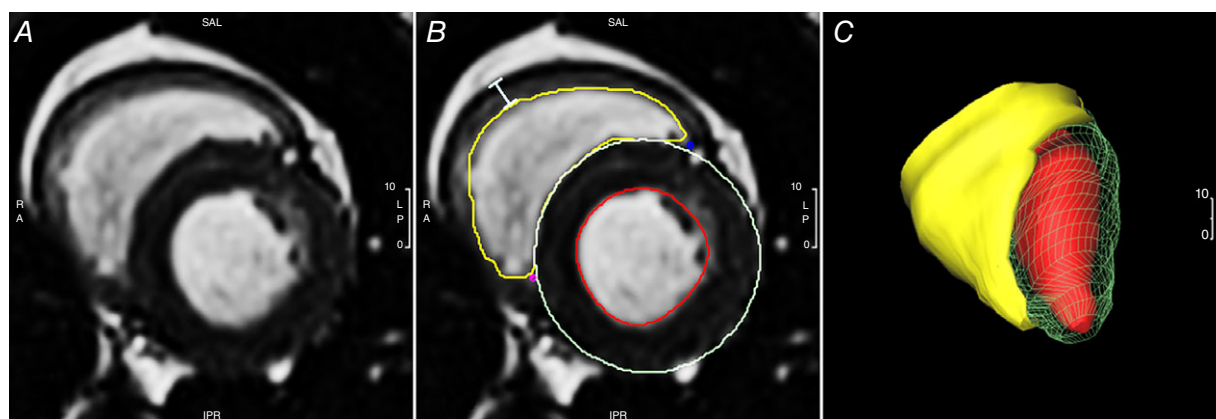


Figure 1. Analysis of CMRI data

For CMRI, short axis images of the ventricles were obtained *en bloc* in a phase-specific manner. *A*, a sample raw image. *B* and *C*, semi-automatic application of endocardial RV contour (*B*) is performed to produce a working RV model for quantification of measurements (*C*). Wall thickness measurement is taken from visually selected representative positions of the right ventricle free wall (bar, *B*). Also shown are the LV tracings previously reported (*B*). [Colour figure can be viewed at wileyonlinelibrary.com]

correlation analyses between RV-EF vs. LSF and RV-EF vs. WTF were completed to establish that both volumetric and structural findings were in agreement. Last, for quality control to assess the internal validity of the measurements, a comparative analysis of LV vs. RV stroke volumes was performed. In correlation assessments, Pearson correlation was performed to evaluate the null hypothesis of no significant associations between parameters within groups, as indicated. Comparison of correlation between groups was performed by one-way ANCOVA as appropriate.

Data are presented as mean \pm standard error of the mean (SEM) unless stated otherwise. In correlation assessments, regression lines are shown as continuous line with dotted 95% confidence bands. Statistical significance was set at $P < 0.05$ for all tests. Asterisks denote significance, detailed in table legends.

Results

Subject baseline characteristics and CMRI timing parameters

For completeness, baseline morphometric data of the various baboon cohorts are recapitulated in Table 1, as previously published (Kuo *et al.* 2016). Male baboons showed higher body weights than females, a known physiological difference that is reflected in the formula used in normalization. A slightly higher resting heart rate was also noted in the female baboons ($P < 0.05$). IUGR birth weights were reduced compared to age-matched controls ($P < 0.01$).

Right ventricular function

The measured RV functional parameters are shown in Table 2. No group–sex interaction was found in any of the measured parameters. ANOVA determined sex to be a significant factor in all volumetric measurements of RV function before normalization, with higher values in male animals in stroke volume, cardiac output, overall ejection rate, early filling rate and overall filling rate. After normalization, sex remained a significant factor only in stroke volume, where a slightly higher value was noted in the males compared to females. When normalized stroke volume was combined with heart rate, the resulting normalized cardiac output was not different between the sexes. Group effect was significant in all RV functional measurements after normalization (Fig. 2) with higher values in the CTL animals than both OLD and IUGR, while OLD and IUGR data were similar.

Right ventricular morphology

RV morphological parameters are shown in Table 3 with ANOVA and *post hoc* results. The RV chamber

volume was higher in males compared to females at both end-systole and end-diastole, and this difference persisted after normalization to BSA. The IUGR animals maintained a higher end-systolic volume than both CTL and OLD. A similar trend was noted in end-diastolic volume, which was only significant between IUGR and OLD. Longitudinal shortening fraction (Fig. 3A) and WTF (Fig. 3B) were decreased in OLD and IUGR animals compared with CTL, while OLD and IUGR were similar. Likewise, normalized peak RV wall thickness was lower in these two groups compared to CTL but not before normalization. The sphericity index at both end-systole (Fig. 3C) and end-diastole (Fig. 3D) was decreased in OLD but unchanged in IUGR.

Correlation and regression

A positive correlation was found between EF and birth weight (Fig. 4A, $R = 0.59$, $P < 0.001$), mainly as a result of group stratification, which presents as clustering by group for both parameters. Individually, the correlation was not significant (CTL $P = 0.16$, IUGR $P = 0.10$). Similarly, a positive correlation was identified between eFR and birth weight (Fig. 4B, $R = 0.59$, $P < 0.001$) secondary to group stratification without individually significant slopes (CTL $P = 0.15$, IUGR $P = 0.15$). There was a positive correlation (Fig. 4C) between RV-EF and LV-EF (Fig. 4C, $R = 0.80$, $P < 0.001$). This positive correlation was seen individually per group (CTL $P < 0.05$, OLD $P < 0.05$, IUGR $P < 0.01$), without difference in slope between groups. RV ejection and filling rates were highly correlated (Fig. 4D, $R = 0.76$, $P < 0.001$). This correlation was seen individually per group (CTL $P < 0.01$, OLD $P < 0.01$, IUGR $P = 0.001$). Lastly, RV-EF was correlated with LSF (Fig. 5A, $R = 0.73$, $P < 0.001$). This correlation was seen individually within groups (CTL $P = 0.03$, OLD $P = 0.02$, IUGR $P = 0.0003$) without between-group differences ($P = 0.43$). The RV-EF was also correlated with WTF (Fig. 5B, $R = 0.75$, $P < 0.001$). This correlation was seen individually within groups (CTL $P = 0.01$, OLD $P = 0.002$, IUGR $P = 0.005$) without between-group differences ($P = 0.38$). As an internal control we performed linear regression between LV and RV stroke volumes, revealing a best-fit line with slope of 0.998 and intercept of 2.6 ($R = 0.86$ and $P < 0.001$).

Discussion

In human studies and in many animal models, including this baboon model, impaired LV heart function has been found to be a consequence of IUGR (Barker, 1995; Crispi *et al.* 2010; Allison *et al.* 2016; Kuo *et al.* 2016). The interdependence of LV and RV function has importance for a variety of cardiac pathologies (Santamore & Dell'Italia, 1998). In the current study, we investigated whether

Table 2. Right ventricular functional parameters (mean \pm SEM)

Parameter	CTL ($n = 16$)	OLD ($n = 12$)	IUGR ($n = 16$)	ANOVA	Post hoc
Absolute values					
RV-SV (ml)	12.6 \pm 1.1	12.1 \pm 2.1	10.7 \pm 1.2	S***	M > F***
Male	14.1 \pm 1.4	17.4 \pm 3.0	14.2 \pm 1.1		
Female	11.2 \pm 1.6	6.8 \pm 0.6	7.2 \pm 1.0		
RV-CO (l min ⁻¹)	1.28 \pm 0.13	1.09 \pm 0.18	1.00 \pm 0.12	S***	M > F***
Male	1.31 \pm 0.13	1.52 \pm 0.25	1.30 \pm 0.14		
Female	1.25 \pm 0.23	0.67 \pm 0.08	0.69 \pm 0.13		
RV-EF (%)	49 \pm 2	39 \pm 3	33 \pm 3	G***	CTL > OLD* CTL > IUGR***
Male	49 \pm 2	38 \pm 5	33 \pm 4		
Female	49 \pm 3	40 \pm 4	33 \pm 4		
RV-ER (ml s ⁻¹)	51.0 \pm 5.5	45.9 \pm 7.8	42.9 \pm 5.2	S***	M > F***
Male	54.5 \pm 5.0	63.5 \pm 11.7	55.9 \pm 6.9		
Female	48.0 \pm 9.5	28.3 \pm 2.8	30.0 \pm 4.6		
RV-eFR (ml s ⁻¹)	50.1 \pm 3.1	39.1 \pm 4.4	22.9 \pm 3.7	G*** S**	CTL > IUGR*** OLD > IUGR** M > F**
Male	54.2 \pm 2.8	50.1 \pm 5.5	27.0 \pm 5.6		
Female	46.5 \pm 5.1	29.8 \pm 3.4	18.9 \pm 4.7		
RV-FR (ml s ⁻¹)	40.0 \pm 4.6	30.7 \pm 5.0	27.3 \pm 3.3	S**	M > F**
Male	42.0 \pm 6.4	42.7 \pm 6.7	35.6 \pm 3.6		
Female	37.6 \pm 6.9	18.8 \pm 2.8	19.0 \pm 3.9		
Normalized to body surface area (BSA)					
RV-SV/BSA (ml/m ²)	26.5 \pm 1.8	17.9 \pm 2.1	20.2 \pm 1.8	G** S**	CTL > OLD** CTL > IUGR* M > F**
Male	28.2 \pm 1.8	22.2 \pm 3.2	24.1 \pm 2.3		
Female	24.9 \pm 3.2	13.6 \pm 1.5	16.4 \pm 2.1		
RV-CO/BSA (l min ⁻¹ m ⁻²)	2.73 \pm 0.27	1.64 \pm 0.18	1.89 \pm 0.20	G**	CTL > OLD** CTL > IUGR*
Male	2.68 \pm 0.23	1.95 \pm 0.27	2.20 \pm 0.25		
Female	2.79 \pm 0.50	1.33 \pm 0.18	1.58 \pm 0.28		
RV-ER/BSA (ml s ⁻¹ m ⁻²)	111 \pm 12	69 \pm 8	81 \pm 8	G*	CTL > OLD* CTL > IUGR-
Male	114 \pm 12	82 \pm 13	94 \pm 11		
Female	108 \pm 22	56 \pm 7	68 \pm 10		
RV-eFR/BSA (ml s ⁻¹ m ⁻²)	109.2 \pm 7.8	62.9 \pm 5.2	44.6 \pm 7.3	G***	CTL > OLD*** CTL > IUGR***
Male	113.6 \pm 10.6	67.3 \pm 6.7	46.3 \pm 10.6		
Female	104.9 \pm 12.1	59.2 \pm 7.9	42.9 \pm 10.6		
RV-FR/BSA (ml s ⁻¹ m ⁻²)	69.3 \pm 4.2	46.0 \pm 5.1	51.9 \pm 5.7	G**	CTL > OLD** CTL > IUGR*
Male	73.8 \pm 5.9	54.6 \pm 6.8	60.4 \pm 6.7		
Female	63.2 \pm 5.5	37.5 \pm 6.1	43.4 \pm 8.7		

G, group only; S, sex only; GS, group and sex; * $P < 0.05$; ** $P < 0.01$; *** $P < 0.005$. No significant sex-group interaction was found. CO, cardiac output; EF, ejection fraction; eFR, early filling rate; ER, ejection rate; FR, filling rate; RV, right ventricular; SV, stroke volume.

declines in RV ejection and filling functions occur in IUGR offspring. We found that the IUGR animals display decreased RV ejection fraction, RV stroke volume, RV cardiac index, RV overall ejection rate, RV early filling rate and RV overall filling rate, consistent with the observed structural changes of decreased longitudinal shortening and decreased wall thickening, sharing many similarities

with OLD animals but also a few key differences (Table 4). Overall, our findings lend further support to our operating hypothesis that perinatal nutrition challenges can result in long-term impaired offspring cardiovascular health. To the best of our knowledge, this is the first study to report impaired RV function in young adulthood in an experimental primate model exposed to developmental

programming through a developmental environment challenge – in this instance decreased maternal nutrient availability during pregnancy and lactation.

This study was motivated by the hypothesis that interdependence of the cardiac ventricles in the setting of known impaired LV function dictates that some impairment must occur in the right ventricle. In the previous study, we found diminished systolic and diastolic LV function in the IUGR and OLD baboons (Kuo *et al.* 2016). The current study found that RV function was more severely impaired than LV function. In the IUGR animals, a 33% reduction in RV-EF was seen while there was a 22% decrease in the LV. In the OLD group, RV-EF was 20% lower compared to 14% in the LV. There was also a more pronounced decline (negative 59%) in early RV filling rate with IUGR compared to the 28% decrease seen in the LV. Interestingly, unlike the impairments occurring in the LV, the deficits in RV function had some dissimilar characteristics for the IUGR and OLD groups.

The RV volumes (ESV/BSA: +55%, EDV/BSA: +14%) and end-diastolic sphericity index increased (+19%) in the IUGR animals relative to CTL, while in the OLD group, the RV volumes remained unchanged and the RV sphericity indices decreased (RV-ESSI –39%, RV-EDSI –21%).

The right ventricle contracts due to a combination of the inward movement of the RV free wall, shortening of the longitudinal fibres, and the effects of LV contraction (Haddad *et al.* 2008b). Normally, longitudinal shortening accounts for the majority of RV contraction (Brown *et al.* 2011), responsible for approximately 80% of the RV stroke volume (Carlsson *et al.* 2007a). Inward radial movement of the RV free wall contributes to 30% of the RV stroke volume, which is partially counteracted by movement of the interventricular septum toward the left ventricle (negative contribution, approximately 10%) (Ostenfeld *et al.* 2016). In the presence of LV dysfunction, at least two features may contribute to the decrease in RV function.

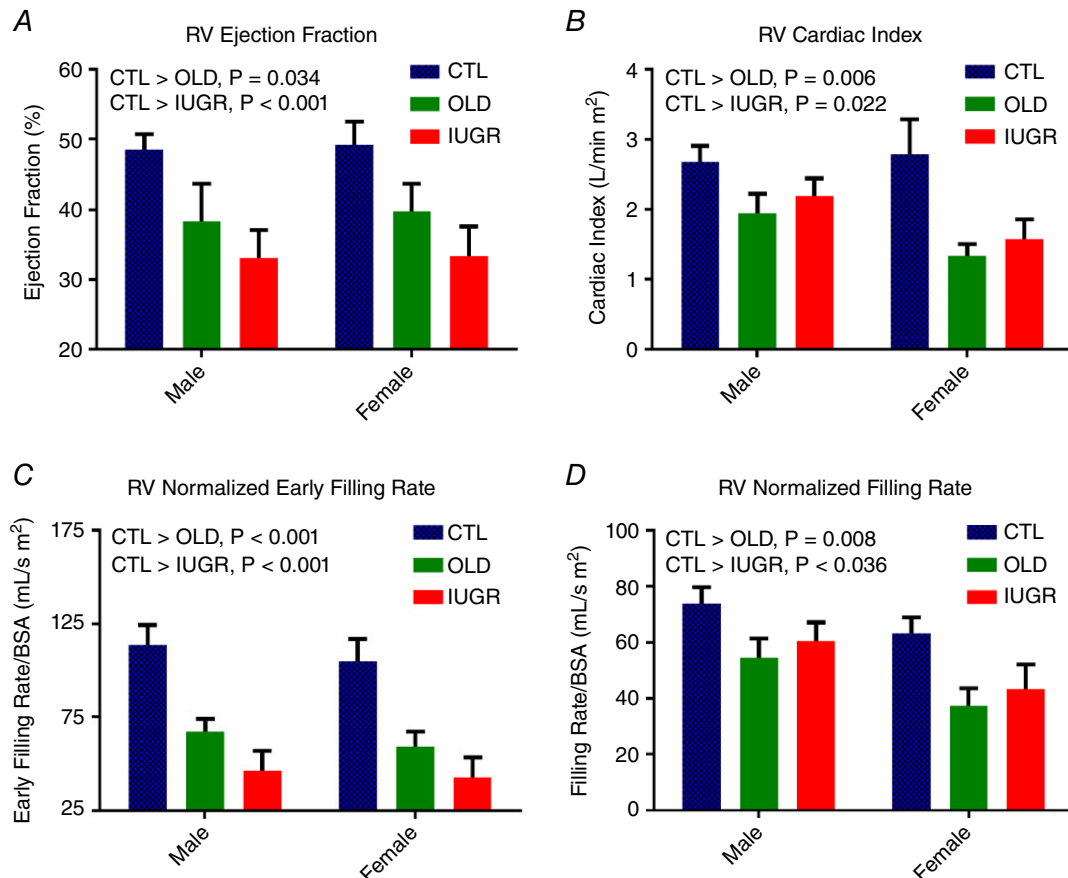


Figure 2. RV ejection and filling rates in CTL, OLD and IUGR baboons

A, decreased RV-EF is seen in both OLD ($P < 0.05$) and IUGR groups ($P < 0.001$) compared to CTL. B, this decrease in ejection fraction is reflected in normalized cardiac output where decreased values are again seen in both OLD ($P < 0.01$) and IUGR ($P < 0.05$). C and D, both eFR (C) and overall filling rate (D) are decreased in OLD (eFR/BSA $P < 0.001$, FR/BSA $P < 0.01$) and IUGR (eFR/BSA $P < 0.001$, FR/BSA $P < 0.05$). No sex difference or group-sex interaction was seen in these four measurements. One outlier was removed from male OLD group in C; two outliers were removed from female CTL group in D. [Colour figure can be viewed at wileyonlinelibrary.com]

Table 3. Right ventricular morphologic parameters (mean \pm SEM)

Parameter	CTL (<i>n</i> = 16)	OLD (<i>n</i> = 12)	IUGR (<i>n</i> = 16)	ANOVA	Post hoc
Absolute values					
RV-ESV (ml)	14.4 \pm 1.7	16.4 \pm 2.5	23.0 \pm 3.1	G** S***	CTL < IUGR** M > F***
Male	17.4 \pm 2.8	23.1 \pm 3.2	31.4 \pm 4.3		
Female	11.4 \pm 1.6	10.7 \pm 1.5	14.5 \pm 1.2		
RV-EDV (ml)	28.0 \pm 3.0	31.7 \pm 5.5	33.7 \pm 3.8	S***	M > F***
Male	33.3 \pm 4.7	45.8 \pm 7.1	45.6 \pm 4.2		
Female	22.6 \pm 2.8	17.6 \pm 1.5	21.7 \pm 1.3		
RV-pWT (mm)	4.1 \pm 0.3	3.2 \pm 0.3	2.9 \pm 0.4	-	
Male	4.7 \pm 0.5	3.7 \pm 0.5	2.6 \pm 0.5		
Female	3.4 \pm 0.4	2.8 \pm 0.2	3.2 \pm 0.6		
RV-LSF (%)	26 \pm 3	17 \pm 2	15 \pm 2	G**	CTL > OLD* CTL > IUGR**
Male	28 \pm 3	16 \pm 3	13 \pm 3		
Female	23 \pm 4	19 \pm 2	17 \pm 2		
RV-WTF (%)	61 \pm 3	45 \pm 4	44 \pm 5	G*	CTL > OLD* CTL > IUGR*
Male	61 \pm 4	50 \pm 8	44 \pm 9		
Female	61 \pm 6	40 \pm 4	43 \pm 6		
RV-ESSI (%)	62 \pm 6	38 \pm 3	63 \pm 5	G**	CTL > OLD* IUGR > OLD*
Male	63 \pm 8	38 \pm 5	60 \pm 5		
Female	61 \pm 9	39 \pm 3	66 \pm 9		
RV-EDSI (%)	48 \pm 4	35 \pm 2	57 \pm 4	G**	CTL > OLD- IUGR > OLD**
Male	43 \pm 5	36 \pm 4	59 \pm 5		
Female	53 \pm 6	34 \pm 2	56 \pm 7		
Normalized to body surface area (BSA)					
RV-ESV/BSA (ml m ⁻²)	27.8 \pm 8.6	28.6 \pm 13.0	43.1 \pm 16.1	G*** S***	CTL < IUGR** OLD < IUGR** M > F***
Male	30.6 \pm 3.1	36.2 \pm 5.5	52.0 \pm 6.2		
Female	25.1 \pm 2.8	21.1 \pm 2.9	33.7 \pm 3.2		
RV-EDV/BSA (ml m ⁻²)	54.4 \pm 3.4	46.5 \pm 4.8	63.1 \pm 4.6	G** S***	OLD < IUGR** M > F***
Male	58.7 \pm 4.5	58.4 \pm 5.9	76.1 \pm 5.7		
Female	50.0 \pm 4.9	34.7 \pm 3.4	50.1 \pm 3.2		
RV-pWT/BSA (mm m ⁻²)	8.4 \pm 0.8	5.4 \pm 0.2	5.9 \pm 0.9	G*	CTL > OLD* CTL > IUGR-
Male	8.9 \pm 1.1	5.3 \pm 0.3	4.7 \pm 0.9		
Female	7.9 \pm 1.1	5.4 \pm 0.3	7.2 \pm 1.4		

G, group only; S, sex only; GS, group and sex; $-P < 0.1$; $*P < 0.05$; $**P < 0.01$; $***P < 0.005$. No significant sex-group interaction was found. EDSI, end diastolic sphericity index; EDV, end diastolic volume; ESSI, end systolic sphericity index; ESV, end systolic volume; LSF, longitudinal shortening fraction; pWT, peak wall thickness; RV, right ventricular; WTF, wall thickening fraction.

First, because longitudinal shortening is also the major contributor to LV pumping (Carlsson *et al.* 2007b) that occurs synergistically with tricuspid pull of the right ventricle, decreased LV function may lead to concurrent decrease in RV longitudinal shortening, impairing RV function. Second, if the decrease in LV longitudinal shortening function is in part compensated by exaggerated septal motion, there may be in effect increased 'steal' of the RV-SV, further lowering RV function.

In both IUGR and OLD groups, reduction in RV fractional longitudinal shortening was seen, thought to be the mechanistic basis of impaired function. Remarkably, the IUGR hearts were able to partially mitigate the effects of reduced RV longitudinal shortening by increasing the RV end-diastolic volume. The increase in ventricular volume in effect partially maintained the RV longitudinal stroke volume by increasing the RV short axis area (Carlsson *et al.* 2007a), similar to the

compensatory changes that preserved ventricular stroke volume previously documented in elderly sedentary humans (Steding-Ehrenborg *et al.* 2015). Additionally, with this increase in preload, some improvement of ejection function occurred in the IUGR hearts via the Frank–Starling mechanism. Those changes were not seen in OLD. Functionally, these changes lead to concomitant decrease in RV ejection fraction and relative preservation of ejection rate/cardiac index in the IUGR group compared to OLD. In their evaluation of the right ventricle in a hypoxia-induced IUGR rat model, Rueda-Clausen *et al.* observed increased RV diameter in the IUGR group at 12 months of age (Rueda-Clausen *et al.* 2009), which may be a related finding of increased preload and RV short axis area. In that study, the increased RV diameter was only significant in the males and not in females, which is analogous to our finding of more

pronounced increase in the male baboons, and represents a potential sexual dimorphism.

RV function has not been investigated to the same extent as LV function, and consequently its importance has been underestimated (Sade & Castaneda, 1975; Rigolin *et al.* 1995). One factor responsible for this relative lack of attention is the difficulty in obtaining its measurements in an accurate and reliable manner (Oldershaw & Bishop, 1995; Grothues *et al.* 2004). The RV chamber, unlike its left counterpart, is not rigidly supported by thick musculature. Consequently, its morphology is often variable, making geometric modelling difficult (Fritz *et al.* 2005; Sheehan & Redington, 2008). Similarly, the relative thinness of the RV wall makes proper wall thickness measurements problematic, at least in humans. While the normally high capacity of the right ventricle gives a broad range of physiological RV-EF (40–76%) in humans depending on the

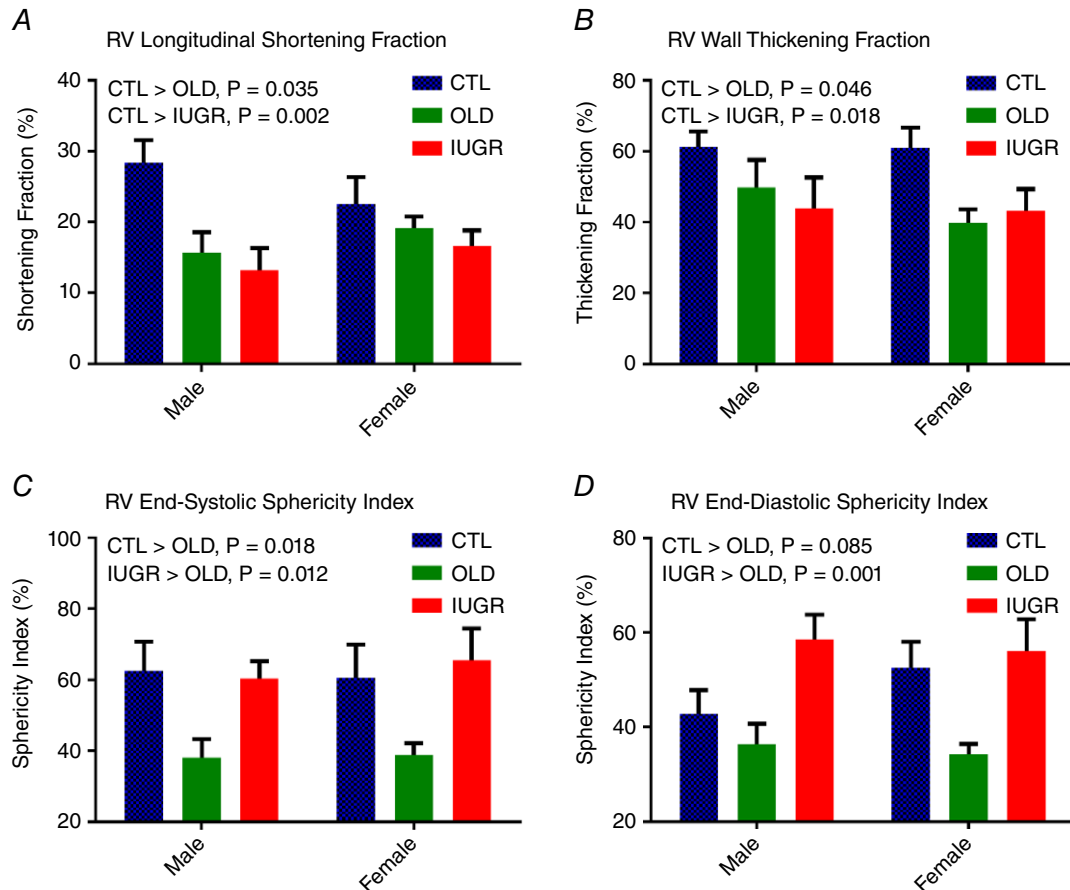


Figure 3. Changes of RV morphology

A, RV longitudinal shortening is decreased in OLD ($P < 0.05$) and IUGR ($P < 0.005$) compared to CTL. B, similarly, RV-WTF is decreased in both OLD ($P < 0.05$) and IUGR ($P < 0.05$) compared to CTL. C and D, RV remodelling occurs in OLD, with both RV sphericity indices decreased at both end-systole (C) and end-diastole (D). In contrast, there is pseudo-normalization of the IUGR sphericity indices secondary to both increased chamber volume and decreased longitudinal shortening. No sex difference or group–sex interaction was seen in these four measurements. One outlier was removed from the male OLD group in both C and D. [Colour figure can be viewed at wileyonlinelibrary.com]

volume status (Haddad *et al.* 2008a), RV dilatation is often the first sign of underlying RV dysfunction (Mertens & Friedberg, 2010). Interestingly, the combination of increased RV-EDV and RV-ESV, preservation of RV-SV and decreased RV-EF we observed in the IUGR baboons also is seen in the setting of pulmonary hypertension (Grapsa *et al.* 2010). Associations between low birth weight and pulmonary hypertension in the neonatal period and pulmonary abnormalities later in life are well documented (Berkelhamer *et al.* 2013; Stocks & Sonnappa, 2013). In extremely low birth weight neonates, pulmonary hypertension and RV dysfunction occur together (Danhaive *et al.* 2005). In the prenatal period, redistribution of cardiac output to the left ventricle in human IUGR fetuses has been reported, thought to be a consequence of increased RV afterload (Watanabe *et al.* 2009). The shift in haemodynamics we observed in the right ventricle suggests that significant RV pressure–volume changes may occur in the setting of IUGR without overt signs and symptoms of right heart dysfunction. These findings raise the concern

that there may be a large unidentified population suffering from adverse RV cardiovascular outcomes resulting from IUGR.

The presence of systolic dysfunction was to be expected. Experimental animal studies show that approximately one-third of RV pressure and outflow result from LV contraction (Yamaguchi *et al.* 1991). RV dysfunction has been demonstrated by Doppler evaluation in human IUGR fetuses showing increased RV Tei index, a myocardial performance index independent of ventricular geometry and heart rate (Tsutsumi *et al.* 1999). Similarly, decreased RV systolic function has been noted in children (mean age of 5 years) with history of IUGR in the form of decreased tricuspid movement (Crispi *et al.* 2010), but not in the detail reported here in our experimental model. Between-species differences are likely to exist as RV systolic function was not decreased in 90- to 120 day-old MNR-induced IUGR rats at baseline, but decreased more severely upon hypoxia challenge in the IUGR group in an echocardiographic study (Keenaghan

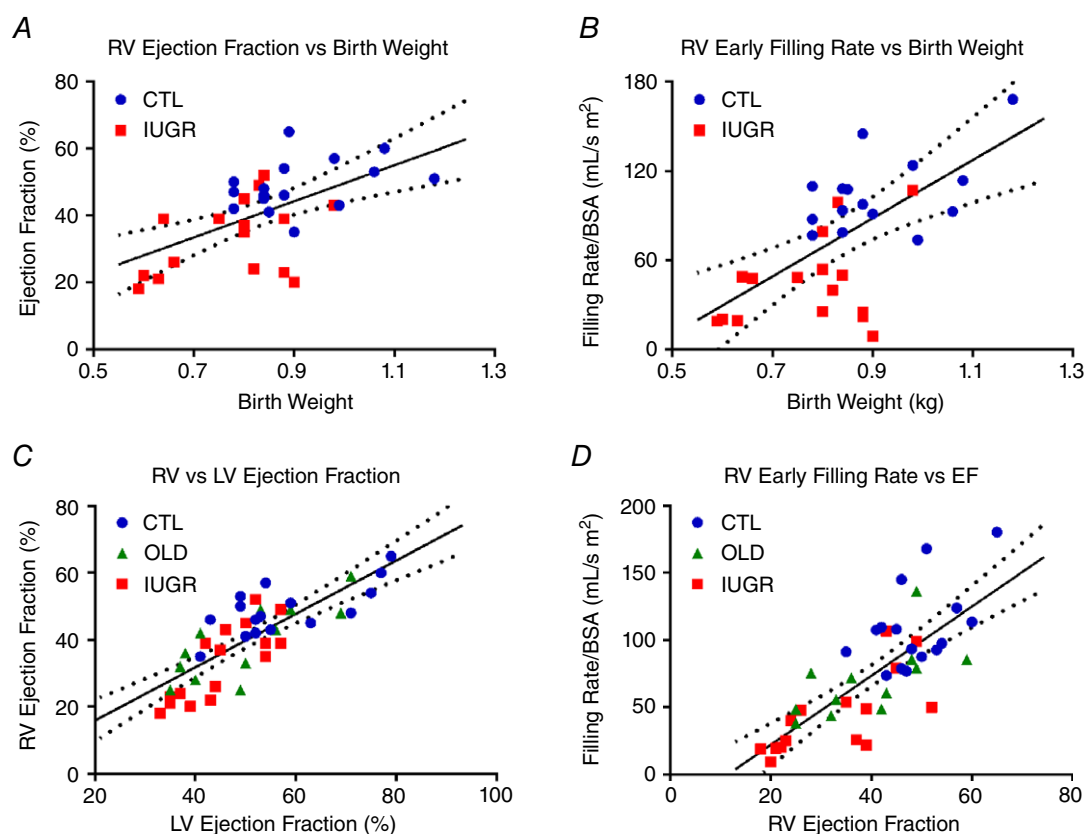


Figure 4. Correlation analyses of RV ejection and filling rates

A, a positive correlation is seen between RV-EF and birth weight ($R = 0.59$, $P < 0.001$) with group stratification. Individually, the correlation is not significant (CTL $P = 0.16$, IUGR $P = 0.10$). B, similarly, a positive correlation is identified between RV-eFR and birth weight ($R = 0.59$, $P < 0.001$). Individually, the correlation is not significant (CTL $P = 0.15$, IUGR $P = 0.15$). C, RV-EF correlates strongly with LV-EF ($R = 0.80$, $P < 0.001$), seen individually per group (CTL $P < 0.05$, OLD $P < 0.05$, IUGR $P < 0.01$). D, RV ejection and filling functions are highly correlated ($R = 0.76$, $P < 0.001$), seen individually per group (CTL $P < 0.01$, OLD $P < 0.01$, IUGR $P = 0.001$). [Colour figure can be viewed at wileyonlinelibrary.com]

et al. 2016). Unexpectedly, in this setting of IUGR offspring we observed more pronounced decline in RV function than LV with strong correlation between the two. Of great importance in relation to aetiology, this shift is contrary to early sparing of the RV function and weaker association typically seen in RV dysfunction secondary to LV dysfunction (Haddad *et al.* 2008*b*). These findings indicate direct effects on RV function in addition to the haemodynamic changes secondary to LV dysfunction. The distinction that a component of RV dysfunction occurs independently of LV abnormality is important because it indicates prospective treatments should consider RV function distinctly to maximize therapeutic potential.

We have previously attributed LV systolic dysfunction in the IUGR baboons at least partly to shortened LV sarcomere length, as documented in human IUGR fetuses (Iruretagoyena *et al.* 2014). There is a need for a similar study on RV sarcomere length in this model. Likewise, we have attributed decreased LV systolic function partially to decreased number of cardiomyocytes from IUGR, as previously suggested in low birth weight 9-week-old sheep (Stacy *et al.* 2009) and low-protein-induced IUGR neonatal rats (Corstius *et al.* 2005). However, a similar correlation between RV cardiomyocyte number and birthweight was not observed in the sheep experiment, and the anatomical source of the cardiomyocytes studied in the rat study was not specified. These issues show the need for further studies in non-human primates. Similarly, delayed cardiomyocyte maturation has been found in the LV but not RV in a placental embolization-induced IUGR fetal sheep model (Bubb *et al.* 2007). Early study on hypobaric hypoxia-induced IUGR newborn rabbits revealed an increase in the RV to LV weight ratio (Chang *et al.* 1984), but the significance of that finding is not clear. A recent study in caloric restriction-induced IUGR

rats (120–180 days old) revealed hypersensitivity of RV mitochondria to oxygen deprivation (Keenaghan *et al.* 2016). Yet, mitochondrial function was unchanged prior to hypoxia in that study, and how this increased sensitivity contributes to long-term cardiac function remains to be studied. Together, these results indicate that further detailed examination of the right ventricle is needed.

In the chick embryo model of chronic hypoxia-induced IUGR, Salinas *et al.* (2014) reported echocardiographic indices of pulmonary hypertension in 6-month-old male IUGR offspring. Echocardiographic evidence of pulmonary hypertension has also been found in a hypoxia IUGR rat model at 12 months of age with increased media thickness in small pulmonary arteries (Rueda-Clausen *et al.* 2009). These reports establish that the RV after-load is likely to have been abnormal, at least at some point in the development of our IUGR baboons. It remains to be seen if the pulmonary hypertension has persisted into later life. It has been suggested that increased vascular burden is seen in IUGR due to an unbalanced growth, as a component of the originally proposed disproportionate fetal growth hypothesis (Barker, 1995). Growth of the body that occurs in IUGR subjects after birth is thought to be unaccompanied by proportional vascular expansion, resulting in increased vascular burden and persistently decreased calibre of the blood vessels (Karatzas & Varvarigou, 2013). If these changes are taking place in the pulmonary vasculature, some degree of elevated pulmonary pressure can be expected to occur, which would partially explain our findings. Additionally, IUGR due to a poor maternal diet has been shown to weaken angiogenesis (Khorram *et al.* 2007) and promote vascular remodelling/stiffening (Dodson *et al.* 2017). Reduction in pulmonary vascular density, impaired pulmonary arterial endothelial function, and decreased

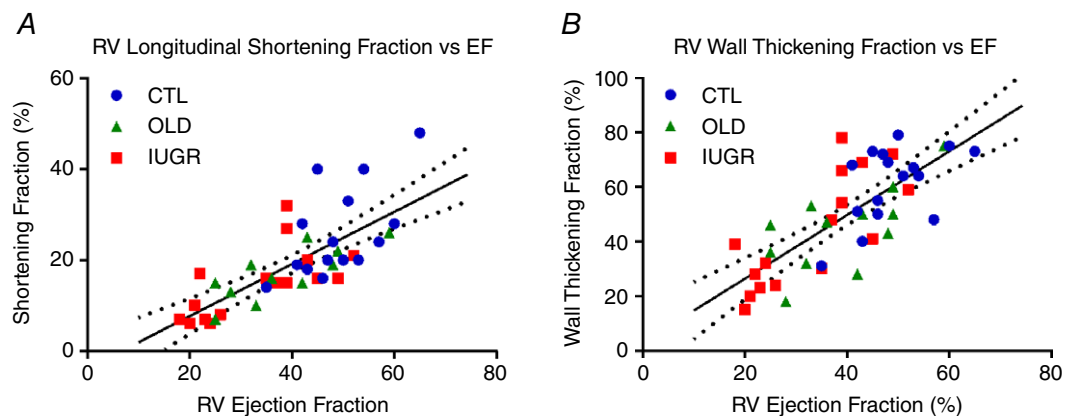


Figure 5. RV longitudinal shortening and wall thickening are associated with RV ejection fraction

A, RV-EF is significantly correlated with RV-LSF ($R = 0.73$, $P < 0.001$). This correlation is seen individually within groups (CTL $P = 0.03$, OLD $P = 0.02$, IUGR $P = 0.0003$) without between-group differences ($P = 0.43$). B, RV-EF also correlates with RV-WTF ($R = 0.75$, $P < 0.001$). This correlation is seen individually within groups (CTL $P = 0.01$, OLD $P = 0.002$, IUGR $P = 0.005$) without between-group differences ($P = 0.38$). [Colour figure can be viewed at wileyonlinelibrary.com]

Table 4. Comparisons between IUGR and OLD groups in RV structure and function and LV structure and function (from Kuo *et al.* 2016)

Measurement	IUGR		OLD	
	LV	RV	LV	RV
Ejection fraction	Decreased	Decreased	Decreased, NS	Decreased
Normalized stroke volume	Decreased, NS	Decreased	Decreased, NS	Decreased
Cardiac index	Decreased	Decreased	Decreased	Decreased
Normalized ejection rate	Decreased, NS	Decreased, NS	Decreased, NS	Decreased
Normalized filling rate	Decreased	Decreased	Decreased	Decreased
Normalized peak wall thickness	Decreased	Decreased, NS	Decreased	Decreased
Wall thickening	Decreased	Decreased	No change	Decreased
Normalized end-systolic volume	Increased	Increased	No change	No change
Normalized end-diastolic volume	No change	Increased	No change	No change
End-systolic sphericity index	Increased	No change	Increased	Decreased
End-diastolic sphericity index	Increased	Increased, NS	Increased	Decreased, NS

pulmonary alveolarization have been documented in a temperature-induced severe placental insufficiency IUGR fetal sheep model (Rozance *et al.* 2011), but it is not clear whether these changes are specific to the method of IUGR induction. Epigenetic studies of MNR-induced IUGR in 1-day-old and 6-week-old rat pulmonary vascular endothelial cells revealed changes that result in increased sensitivity to hypoxia later in life that may be partially responsible for higher likelihood of pulmonary hypertension and vascular remodelling (Xu *et al.* 2013). In aggregate, these studies support our interpretation that the presence of pulmonary hypertension may underlie IUGR RV dysfunction, and may explain the few differences in RV function and morphology we observed between IUGR and OLD. Echocardiographic studies of normal human subjects unveil only modest pulmonary artery systolic pressure increases with age without overt pulmonary hypertension (McQuillan *et al.* 2001; Lam *et al.* 2009a). Notably, it is known that the right ventricle experiences heightened sensitivity to afterload change compared to the left ventricle (Chin *et al.* 2005), which may explain the higher degree of decrease in RV function in the IUGR cohort compared to the extent of decrease in LV function. In future studies we plan to determine whether significant differences in pulmonary vascular calibre and hypertension are present in our cohort, and if so, whether alleviation of pulmonary hypertension is sufficient to rescue RV function.

Compared to the relative preservation of ejection rate, the decline in filling function with IUGR was more prominent, with more than 50% reduction in active filling rate. There was a subsequent shift toward higher degree of passive RV filling, resulting in a less affected overall filling rate. This predominant diastolic failure in IUGR has previously been noted in the hypoxia-induced chick embryo model (Itani *et al.* 2016). Decreased RV diastolic function has been noted in children with history of IUGR (Crispi

et al. 2010). In that echocardiographic study, prolonged RV active phase deceleration time, decreased tricuspid annular movement during early diastole, and a trend of decreased tricuspid E/A ratio was seen, consistent with blunting of active filling. Our findings again indicate that those unfavourable changes present in IUGR continue into adulthood in our primate model. While evaluation of the filling function is difficult in the presence of ejection dysfunction, we would hypothesize that at least three factors are in play. First, the increased chamber volume that is thought to be responsible for relative preservation of the ejection function is likely to contribute to decreased filling function. Second, the filling duration is a significant determinant of RV filling function (Dell'Italia, 1990) with RV filling beginning before and ending after LV filling (Haddad *et al.* 2008a). Therefore, the shortened diastole we have reported is likely to contribute to poor filling function (Kuo *et al.* 2016). Last, we suspect decreased RV compliance secondary to RV myocardial fibrosis leading to decreased filling function. We have previously identified increased myocardial fibrosis in an IUGR sheep model (Ge *et al.* 2013) and the LV myocardium of our fetal male IUGR baboon cohort (Maloyan *et al.* 2014). Combined, these observations suggest multiple mechanisms are likely to underlie the impaired diastolic RV function, but also that several different strategies will need to be investigated to improve RV filling function.

Our RV morphology measurements were consistent with our functional findings. We detected decreased LSF (Fig. 3A) and WTF (Fig. 3B) in the IUGR and OLD groups alike. Correlation analyses indicated these two measurements are likely to reflect, and may even be the cause of, the decreased ejection function (Fig. 4). The more interesting results arise from our sphericity measurements. We observed decreased RV sphericity indices in the OLD animals at both end-systole and end-diastole, with only a small difference in RV-EDSI between CTL and IUGR.

This difference in sphericity index may arise from the preservation of chamber volume in the OLD animals *versus* the relative chamber distention in the IUGR animals, which coupled with decreased longitudinal shortening results in paradoxical normalization of the sphericity index in IUGR. Supporting our hypothesis regarding increased RV afterload, an increased RV sphericity index is known to occur with pulmonary hypertension (Grapsa *et al.* 2012). In a previous comparison of ageing and programming effects, Allison *et al.* (2016) concluded that ageing is similar to programming in some processes but not others. In that regard, our results suggest that the effects of IUGR and ageing may be distinguished from one another morphologically via chamber volume and sphericity or physiologically via examination of the pulmonary pressure.

The strong similarity of RV and LV stroke volumes, a known physiological constraint, indicates our measurement model is internally consistent. A small amount of positive deviation was observed, indicating a slightly increased LV stroke volume compared to RV, which is consistent with measurement errors reported in previous CMRI human studies (Lorenz *et al.* 1999; Maceira *et al.* 2006). Also, even though our evaluation was performed under anaesthesia using ketamine and isoflurane, which are known to produce fewer effects on cardiovascular depression than other commonly used aesthetic agents (Kazama & Ikeda, 1988; Stowe *et al.* 1992; Oguchi *et al.* 1995), we recognize that our findings may be complicated by differential effects of anaesthetics on IUGR or ageing physiology. In particular, it is possible that variation in sympathetic tone plays a role in the observed cardiac functional irregularity, as previously explored by Lee *et al.* (1998). In addition, we acknowledge that this is a resting study and therefore not wholly representative of cardiovascular function. It is known that cardiovascular function may appear normal at rest but become depressed during periods of increased cardiac demand in certain scenarios. For example, LV ejection fraction remains grossly normal at rest with age, but peak ejection fraction is decreased with exercise in the older population (Port *et al.* 1980; Schulman *et al.* 1992). Without stress studies, it is difficult to gauge the extent of RV functional abnormality in our cohort. We acknowledge that this examination captures only a single time point in the IUGR lifespan. We plan to maintain these interesting cohorts and conduct further studies to determine whether the abnormalities reported here persist and even increase with age in these IUGR animals. Furthermore, we intend to uncover with our subsequent studies whether the findings we report may be complicated by delay in development previously documented with IUGR (Engelbregt *et al.* 2000). As a result, one of the limitations of the study is the inability to test the molecular and cellular pathways involved. Last, we note that our model of maternal undernutrition continues

to the end of lactation. The continuation of maternal nutrient restriction into the neonatal period likely hinders or delays catch-up growth typically observed with IUGR models. Literature suggests catch-up growth as an important factor in alteration of cardiovascular phenotype and that if maternal undernutrition was limited to the prenatal period, a more pronounced impairment of cardiac function may be seen.

In summary, this study demonstrated that RV systolic and diastolic abnormalities occur with IUGR. This suggests increased CVD risk in these IUGR subjects, with subclinical changes that are cause for concern because they show reduced cardiac reserve. It will be useful to determine, with the abnormal IUGR physiology, whether a combination of ageing and additional subclinical challenges, such as stress, may result in overt clinical dysfunction. In addition, the complex interaction among vascular calibre, flow alteration and cardiac dysfunction warrants further investigation. In particular, future studies should explore how pulmonary vascular health impacts RV afterload in IUGR offspring. In addition to estimation of the pulmonary pressure, evaluation of the right atrial volume (Ostenfeld *et al.* 2017), RV outflow tract blood flow waveform (Arkles *et al.* 2011), pulmonic valve motion (Weyman *et al.* 1974) and interventricular septal motion (Jessup *et al.* 1987) may provide further insight into RV pulmonary haemodynamics.

References

- Allison BJ, Kaandorp JJ, Kane AD, Camm EJ, Lusby C, Cross CM, Nevin-Dolan R, Thakor AS, Derks JB, Tarry-Adkins JL, Ozanne SE & Giussani DA (2016). Divergence of mechanistic pathways mediating cardiovascular aging and developmental programming of cardiovascular disease. *FASEB J* **30**, 1968–1975.
- Arkles JS, Opotowsky AR, Ojeda J, Rogers F, Liu T, Prassana V, Marzec L, Palevsky HI, Ferrari VA & Forfia PR (2011). Shape of the right ventricular Doppler envelope predicts hemodynamics and right heart function in pulmonary hypertension. *Am J Respir Crit Care Med* **183**, 268–276.
- Armitage JA, Khan IY, Taylor PD, Nathanielsz PW & Poston L (2004). Developmental programming of the metabolic syndrome by maternal nutritional imbalance: how strong is the evidence from experimental models in mammals? *J Physiol* **561**, 355–377.
- Barker DJ (1995). Fetal origins of coronary heart disease. *BMJ* **311**, 171–174.
- Berkelhamer SK, Mestan KK & Steinhorn RH (2013). Pulmonary hypertension in bronchopulmonary dysplasia. *Semin Perinatol* **37**, 124–131.
- Brown SB, Raina A, Katz D, Szerlip M, Wieggers SE & Forfia PR (2011). Longitudinal shortening accounts for the majority of right ventricular contraction and improves after pulmonary vasodilator therapy in normal subjects and patients with pulmonary arterial hypertension. *Chest* **140**, 27–33.

- Bubb KJ, Cock ML, Black MJ, Dodic M, Boon W, Parkington HC, Harding R & Tare M (2007). Intrauterine growth restriction delays cardiomyocyte maturation and alters coronary artery function in the fetal sheep. *J Physiol* **578**, 871–881.
- Carlsson M, Ugander M, Heiberg E & Arheden H (2007a). The quantitative relationship between longitudinal and radial function in left, right, and total heart pumping in humans. *Am J Physiol Heart Circ Physiol* **293**, H636–H644.
- Carlsson M, Ugander M, Mosen H, Buhre T & Arheden H (2007b). Atrioventricular plane displacement is the major contributor to left ventricular pumping in healthy adults, athletes, and patients with dilated cardiomyopathy. *Am J Physiol Heart Circ Physiol* **292**, H1452–H1459.
- Chang J, Rutledge JC, Stoops D & Abbe R (1984). Hypobaric hypoxia-induced intrauterine growth retardation. *Biol Neonate* **46**, 10–14.
- Chin KM, Kim NH & Rubin LJ (2005). The right ventricle in pulmonary hypertension. *Coron Artery Dis* **16**, 13–18.
- Clarren SK & Smith DW (1978). The fetal alcohol syndrome. *N Engl J Med* **298**, 1063–1067.
- Corstius HB, Zimanyi MA, Maka N, Herath T, Thomas W, Van Der Laarse A, Wreford NG & Black MJ (2005). Effect of intrauterine growth restriction on the number of cardiomyocytes in rat hearts. *Pediatr Res* **57**, 796–800.
- Crispi F, Bijmens B, Figueras F, Bartrons J, Eixarch E, Le Noble F, Ahmed A & Gratacos E (2010). Fetal growth restriction results in remodeled and less efficient hearts in children. *Circulation* **121**, 2427–2436.
- Danhaive O, Margossian R, Geva T & Kourembanas S (2005). Pulmonary hypertension and right ventricular dysfunction in growth-restricted, extremely low birth weight neonates. *J Perinatol* **25**, 495–499.
- de Groote P, Millaire A, Foucher-Hossein C, Nogue O, Marchandise X, Ducloux G & Lablanche J (1998). Right ventricular ejection fraction is an independent predictor of survival in patients with moderate heart failure. *J Am Coll Cardiol* **32**, 948–954.
- Dell'Italia LJ (1990). Mechanism of postextrasystolic potentiation in the right ventricle. *Am J Cardiol* **65**, 736–741.
- Dodson B, Miller T, Powers K, Yang Y, Yu B, Albertine K & Zinkhan E (2017). Intrauterine growth restriction influences vascular remodeling and stiffening in the weanling rat more than sex or diet. *Am J Physiol Heart Circ Physiol* **312**, H250–H264.
- Drazner MH, Hamilton MA, Fonarow G, Creaser J, Flavell C & Stevenson LW (1999). Relationship between right and left-sided filling pressures in 1000 patients with advanced heart failure. *J Heart Lung Transplant* **18**, 1126–1132.
- Engelbregt MJ, Houdijk ME, Popp-Snijders C & Delemarre-van de Waal HA (2000). The effects of intra-uterine growth retardation and postnatal undernutrition on onset of puberty in male and female rats. *Pediatr Res* **48**, 803–807.
- Fowden AL, Giussani DA & Forhead AJ (2006). Intrauterine programming of physiological systems: causes and consequences. *Physiology (Bethesda)* **21**, 29–37.
- Fritz J, Solaiyappan M, Tandri H, Bomma C, Genc A, Claussen CD, Lima JA & Bluemke DA (2005). Right ventricle shape and contraction patterns and relation to magnetic resonance imaging findings. *J Comput Assist Tomogr* **29**, 725–733.
- Ge W, Hu N, George LA, Ford SP, Nathanielsz PW, Wang X & Ren J (2013). Maternal nutrient restriction predisposes ventricular remodeling in adult sheep offspring. *J Nutr Biochem* **24**, 1258–1265.
- Glassman DM, Coelho AM Jr, Carey KD & Bramblett CA (1984). Weight growth in savannah baboons: a longitudinal study from birth to adulthood. *Growth* **48**, 425–433.
- Godfrey KM, Lillycrop KA, Burdge GC, Gluckman PD & Hanson MA (2007). Epigenetic mechanisms and the mismatch concept of the developmental origins of health and disease. *Pediatr Res* **61**, 5R–10R.
- Grapsa J, Gibbs JS, Cabrita IZ, Watson GF, Pavlopoulos H, Dawson D, Gin-Sing W, Howard LS & Nihoyannopoulos P (2012). The association of clinical outcome with right atrial and ventricular remodelling in patients with pulmonary arterial hypertension: study with real-time three-dimensional echocardiography. *Eur Heart J Cardiovasc Imaging* **13**, 666–672.
- Grapsa J, O'Regan DP, Pavlopoulos H, Durighel G, Dawson D & Nihoyannopoulos P (2010). Right ventricular remodelling in pulmonary arterial hypertension with three-dimensional echocardiography: comparison with cardiac magnetic resonance imaging. *Eur J Echocardiogr* **11**, 64–73.
- Grothues F, Moon JC, Bellenger NG, Smith GS, Klein HU & Pennell DJ (2004). Interstudy reproducibility of right ventricular volumes, function, and mass with cardiovascular magnetic resonance. *Am Heart J* **147**, 218–223.
- Grundy D (2015). Principles and standards for reporting animal experiments in *The Journal of Physiology and Experimental Physiology*. *J Physiol* **593**, 2547–2549.
- Haddad F, Doyle R, Murphy DJ & Hunt SA (2008b). Right ventricular function in cardiovascular disease, part II: pathophysiology, clinical importance, and management of right ventricular failure. *Circulation* **117**, 1717–1731.
- Haddad F, Hunt SA, Rosenthal DN & Murphy DJ (2008a). Right ventricular function in cardiovascular disease, Part I: Anatomy, physiology, aging, and functional assessment of the right ventricle. *Circulation* **117**, 1436–1448.
- Iruetagoiena JI, Gonzalez-Tendero A, Garcia-Canadilla P, Amat-Roldan I, Torre I, Nadal A, Crispi F & Gratacos E (2014). Cardiac dysfunction is associated with altered sarcomere ultrastructure in intrauterine growth restriction. *Obstet Gynecol* **210**, 550.e1–550.e7.
- Itani N, Skeffington KL, Beck C, Niu Y & Giussani DA (2016). Melatonin rescues cardiovascular dysfunction during hypoxic development in the chick embryo. *J Pineal Res* **60**, 16–26.
- Jessup M, Sutton MSJ, Weber KT & Janicki JS (1987). The effect of chronic pulmonary hypertension on left ventricular size, function, and interventricular septal motion. *Am Heart J* **113**, 1114–1122.
- Kalogeropoulos AP, Vega JD, Smith AL & Georgiopoulou VV (2011). Pulmonary hypertension and right ventricular function in advanced heart failure. *Congestive Heart Failure* **17**, 189–198.

- Karatzas AA & Varvarigou A (2013). Intrauterine growth restriction and the developing vascular tree. In *Early Life Nutrition and Adult Health and Development: Lessons from Changing Dietary Patterns, Famines and Experimental Studies*, ed. Lumey LH & Vaiserman A. Nova Science Publishers, New York, 331–351.
- Kazama T & Ikeda K (1988). The comparative cardiovascular effects of sevoflurane with halothane and isoflurane. *J Anesth* **2**, 63–68.
- Keenaghan M, Sun L, Wang A, Hyodo E, Homma S & Ten VS (2016). Intrauterine growth restriction impairs right ventricular response to hypoxia in adult male rats. *Pediatr Res* **80**, 547–553.
- Khorram O, Khorram N, Momeni M, Han G, Halem J, Desai M & Ross MG (2007). Maternal undernutrition inhibits angiogenesis in the offspring: a potential mechanism of programmed hypertension. *Am J Physiol Regul Integr Comp Physiol* **293**, R745–R753.
- Kim H, Kim Y, Park J, Kim KH, Kim K, Ahn H, Sohn D, Oh B, Park Y & Choi Y (2006). Determinants of the severity of functional tricuspid regurgitation. *Am J Cardiol* **98**, 236–242.
- Kuo AH, Li C, Li J, Huber HF, Nathanielsz PW & Clarke GD (2016). Cardiac remodelling in a baboon model of intrauterine growth restriction mimics accelerated ageing. *J Physiol* **595**, 1093–1110.
- Lam CS, Borlaug BA, Kane GC, Enders FT, Rodeheffer RJ & Redfield MM (2009a). Age-associated increases in pulmonary artery systolic pressure in the general population. *Circulation* **119**, 2663–2670.
- Lam CS, Roger VL, Rodeheffer RJ, Borlaug BA, Enders FT & Redfield MM (2009b). Pulmonary hypertension in heart failure with preserved ejection fraction: a community-based study. *J Am Coll Cardiol* **53**, 1119–1126.
- Lee J, Park K, Hwang J, Park M & Yum M (1998). Chaotic and periodic heart rate dynamics in uncomplicated intrauterine growth restricted fetuses. *Early Hum Dev* **53**, 121–128.
- Li C, Ramahi E, Nijland MJ, Choi J, Myers DA, Nathanielsz PW & McDonald TJ (2013). Up-regulation of the fetal baboon hypothalamo-pituitary-adrenal axis in intrauterine growth restriction: coincidence with hypothalamic glucocorticoid receptor insensitivity and leptin receptor down-regulation. *Endocrinology* **154**, 2365–2373.
- Lorenz CH, Walker ES, Morgan VL, Klein SS & Graham TP (1999). Normal human right and left ventricular mass, systolic function, and gender differences by cine magnetic resonance imaging. *J Cardiovasc Magn Reson* **1**, 7–21.
- Maceira AM, Prasad SK, Khan M & Pennell DJ (2006). Reference right ventricular systolic and diastolic function normalized to age, gender and body surface area from steady-state free precession cardiovascular magnetic resonance. *Eur Heart J* **27**, 2879–2888.
- Maloyan A, Muralimanoharan S, Nijland M & Nathanielsz PW (2014). Sexual dimorphism in cardiac response to intrauterine growth restriction (IUGR). *Circulation* **130**, A15515.
- McQuillan BM, Picard MH, Leavitt M & Weyman AE (2001). Clinical correlates and reference intervals for pulmonary artery systolic pressure among echocardiographically normal subjects. *Circulation* **104**, 2797–2802.
- Melenovsky V, Hwang SJ, Lin G, Redfield MM & Borlaug BA (2014). Right heart dysfunction in heart failure with preserved ejection fraction. *Eur Heart J* **35**, 3452–3462.
- Mertens LL & Friedberg MK (2010). Imaging the right ventricle—current state of the art. *Nat Rev Cardiol* **7**, 551–563.
- Oguchi T, Kashimoto S, Yamaguchi T, Nakamura T & Kumazawa T (1995). Comparative effects of halothane, enflurane, isoflurane and sevoflurane on function and metabolism in the ischaemic rat heart. *Br J Anaesth* **74**, 569–575.
- Oldershaw P & Bishop A (1995). The difficulties of assessing right ventricular function. *Br Heart J* **74**, 99–100.
- Ostenfeld E, Stephensen S, Steding-Ehrenborg K, Heiberg E, Arheden H, Rådegran G, Holm J & Carlsson M (2016). Regional contribution to ventricular stroke volume is affected on the left side, but not on the right in patients with pulmonary hypertension. *Int J Cardiovasc Imaging* **32**, 1243–1253.
- Ostenfeld E, Werther-Evaldsson A, Engblom H, Ingvarsson A, Roijer A, Meurling C, Holm J, Rådegran G & Carlsson M (2017). Discriminatory ability of right atrial volumes with two- and three-dimensional echocardiography to detect elevated right atrial pressure in pulmonary hypertension. *Clin Physiol Funct Imaging* (in press; <https://doi.org/10.1111/cpf.12398>).
- Oudiz RJ (2007). Pulmonary hypertension associated with left-sided heart disease. *Clin Chest Med* **28**, 233–241.
- Polak JF, Holman BL, Wynne J & Colucci WS (1983). Right ventricular ejection fraction: an indicator of increased mortality in patients with congestive heart failure associated with coronary artery disease. *J Am Coll Cardiol* **2**, 217–224.
- Port S, Cobb FR, Coleman RE & Jones RH (1980). Effect of age on the response of the left ventricular ejection fraction to exercise. *N Engl J Med* **303**, 1133–1137.
- Rigolin VH, Robiolio PA, Wilson JS, Harrison JK & Bashore TM (1995). The forgotten chamber: the importance of the right ventricle. *Cathet Cardiovasc Diagn* **35**, 18–28.
- Roseboom TJ, Van Der Meulen JHP, Ravelli AC, Osmond C, Barker DJ & Bleker OP (2001). Effects of prenatal exposure to the Dutch famine on adult disease in later life: an overview. *Mol Cell Endocrinol* **185**, 93–98.
- Rozance PJ, Seedorf GJ, Brown A, Roe G, O'Meara MC, Gien J, Tang JR & Abman SH (2011). Intrauterine growth restriction decreases pulmonary alveolar and vessel growth and causes pulmonary artery endothelial cell dysfunction in vitro in fetal sheep. *Am J Physiol Lung Cell Mol Physiol* **301**, L860–L871.
- Rueda-Clausen CF, Morton JS & Davidge ST (2009). Effects of hypoxia-induced intrauterine growth restriction on cardiopulmonary structure and function during adulthood. *Cardiovasc Res* **81**, 713–722.
- Sade RM & Castaneda AR (1975). The dispensable right ventricle. *Surgery* **77**, 624–631.
- Salinas CE, Blanco CE, Villena M & Giussani DA (2014). High-altitude hypoxia and echocardiographic indices of pulmonary hypertension in male and female chickens at adulthood. *Circ J* **78**, 1459–1464.

- Santamore WP & Dell'Italia LJ (1998). Ventricular interdependence: significant left ventricular contributions to right ventricular systolic function. *Prog Cardiovasc Dis* **40**, 289–308.
- Schlabritz-Loutsevitch NE, Howell K, Rice K, Glover EJ, Nevill CH, Jenkins SL, Cummins LB, Frost PA, McDonald TJ & Nathanielsz PW (2004). Development of a system for individual feeding of baboons maintained in an outdoor group social environment. *J Med Primatol* **33**, 117–126.
- Schulman SP, Lakatta EG, Fleg JL, Lakatta L, Becker LC & Gerstenblith G (1992). Age-related decline in left ventricular filling at rest and exercise. *Am J Physiol Heart Circ Physiol* **263**, H1932–H1938.
- Segers VF, Brutsaert DL & De Keulenaer GW (2012). Pulmonary hypertension and right heart failure in heart failure with preserved left ventricular ejection fraction: pathophysiology and natural history. *Curr Opin Cardiol* **27**, 273–280.
- Sheehan F & Redington A (2008). The right ventricle: anatomy, physiology and clinical imaging. *Heart* **94**, 1510–1515.
- Stacy V, De Matteo R, Brew N, Sozo F, Probyn ME, Harding R & Black MJ (2009). The influence of naturally occurring differences in birthweight on ventricular cardiomyocyte number in sheep. *Anat Rec* **292**, 29–37.
- Steding-Ehrenborg K, Boushel RC, Calbet JA, Åkeson P & Mortensen SP (2015). Left ventricular atrioventricular plane displacement is preserved with lifelong endurance training and is the main determinant of maximal cardiac output. *J Physiol* **593**, 5157–5166.
- Stocks J & Sonnappa S (2013). Early life influences on the development of chronic obstructive pulmonary disease. *Thorax* **7**, 161–173.
- Stowe DF, Bosnjak ZJ & Kampine JP (1992). Comparison of etomidate, ketamine, midazolam, propofol, and thiopental on function and metabolism of isolated hearts. *Anesth Analg* **74**, 547–558.
- Tsutsumi T, Ishii M, Eto G, Hota M & Kato H (1999). Serial evaluation for myocardial performance in fetuses and neonates using a new Doppler index. *Pediatr Int* **41**, 722–727.
- VandeBerg JL, Williams-Blangero S & Tardif SD (2009). *The Baboon in Biomedical Research*. Springer, New York.
- Voelkel NF, Quaife RA, Leinwand LA, Barst RJ, McGoon MD, Meldrum DR, Dupuis J, Long CS, Rubin LJ, Smart FW, Suzuki YJ, Gladwin M, Denholm EM, Gail DB; National Heart, Lung, and Blood Institute Working Group on Cellular and Molecular Mechanisms of Right Heart Failure (2006). Right ventricular function and failure: report of a National Heart, Lung, and Blood Institute working group on cellular and molecular mechanisms of right heart failure. *Circulation* **114**, 1883–1891.
- Watanabe S, Hashimoto I, Saito K, Watanabe K, Hirono K, Uese K, Ichida F, Saito S, Miyawaki T & Niemann P (2009). Characterization of ventricular myocardial performance in the fetus by tissue Doppler imaging. *Circ J* **73**, 943–947.
- Weyman AE, Dillon JC, Feigenbaum H & Chang S (1974). Echocardiographic patterns of pulmonic valve motion with pulmonary hypertension. *Circulation* **50**, 905–910.
- Xu X, Lv Y, Gu W, Tang L, Wei J, Zhang L & Du L (2013). Epigenetics of hypoxic pulmonary arterial hypertension following intrauterine growth retardation rat: epigenetics in PAH following IUGR. *Respir Res* **14**, 20.
- Yamaguchi S, Harasawa H, Li KS, Zhu D & Santamore WP (1991). Comparative significance in systolic ventricular interaction. *Cardiovasc Res* **25**, 774–783.

Additional information

Competing interests

The authors have no potential conflict of interest, financial or otherwise, to disclose.

Author contributions

A.H.K. participated in the design of the work, the acquisition, analysis and interpretation of data, drafting the manuscript, and revising it critically for important intellectual content. C.L. participated in the development of the IUGR model, design of the work, data acquisition and revising the manuscript critically for important intellectual content. H.F.H. participated in the design of the work, data acquisition and analysis, and revising the manuscript critically for important intellectual content. M.S. participated in the design of the work, data acquisition and analysis, and revising the manuscript critically for important intellectual content. P.W.N. participated in the development of the IUGR model, conception and design of the work, interpretation of data, and revising the manuscript critically for important intellectual content. G.D.C. participated in the conception and design of the work, data analysis, interpretation of data, and writing and revising the manuscript. All authors approved the final version of the manuscript, agree to be accountable for all aspects of the work in ensuring that questions related to the accuracy or integrity of any part of the work are appropriately investigated and resolved, and all persons designated as authors qualify for authorship and all those who qualify for authorship are listed.

Funding

This work was supported by the National Institutes of Health 5P01HD021350 (P.W.N.), 5R24OD011183 (P.W.N.), 5K25DK089012 (G.D.C.), and 1R25EB016631 (A.H.K.). NIH grant OD P51 OD011133 was from the Office of Research Infrastructure Programs/Office of the Director. This work was also supported in part by funding from the EU FP 7/HEALTH/GA No. 279281: BrainAge – Impact of Prenatal Stress on BRAINAGEing.

Acknowledgements

The authors thank Dr Robert Lanford and the Southwest National Primate Center Staff for their ongoing support of the baboon research programme described in this article. The authors also acknowledge the technical support of Steven Rios, Sam Vega and Susan Jenkins, as well as the administrative support of Karen Moore.